JOURNAL OF CATALYSIS 63, 372–382 (1980)

Structure–Property Relations of Solid Polymeric Catalysts: Isopropyl Alcohol Dehydration in Semicrystalline, Sulfonated Polyethylene-Grafted Styrene

C. A. COOPER,[1] R. L. MCCULLOUGH, B. C. GATES[2] AND J. C. SEFERIS*

Center for Catalytic Science and Technology, Department of Chemical Engineering, University of Delaware, Newark, Delaware 19711

** Department of Chemical Engineering, University of Washington, Seattle, Washington 98105*

Received April 13, 1979; revised January 14, 1980

The dehydration of isopropyl alcohol to give propylene was used as a test reaction to measure effects of structural changes on the catalytic activity of semicrystalline polyethylene containing grafted, sulfonated styrene. Structural changes in polymer films were induced by drawing. Catalytic reaction rates were measured with variously drawn polymer films clamped in a differential flow reactor operated at 100°C and 1 atm. The activity of the catalyst and the form of the kinetics were nearly the same as those observed previously with sulfonated poly(styrene–divinylbenzene) catalysts. These results and infrared spectra of the latter catalysts indicate the involvement of several hydrogen-bonded $-SO_3H$ groups in a catalytic site. The catalytic activity increased with drawing of the polymer up to 250% of the initial length; the activity decreased upon further drawing. The polymer structure was characterized as a function of the draw ratio by X-ray diffraction, dynamic mechanical measurements, electron microscopy, and birefringence and density measurements. These quantitative characterizations support the following model for the influence of draw-induced structural changes on catalytic activity. In the undrawn state, there is clustering of hydrogen-bonded $-SO_3H$ groups, all of which are confined to the amorphous regions of the polymer. Initial elongation partially breaks up the clusters, allowing more $-SO_3H$ groups to bond to alcohol and become catalytically engaged. Drawing beyond 250% leads to a separation of $-SO_3H$ groups greater than that for efficient clustering and consequently suppresses the efficient (concerted) reaction involving several acid groups.

INTRODUCTION

Semicrystalline polymers have a hierarchy of molecular and micro structures which are sensitive to the state of deformation of the material. This class of catalyst supports provides the opportunity for simply inducing significant structural variations so that the influence of structure on catalytic behavior can be examined. We report here the results of catalytic activity measurements of a series of sulfonated, semicrystalline polyethylene films in which the structure was systematically varied by drawing.

On the molecular level, the catalyst consists of a polyethylene backbone with sulfonated styrene units grafted onto the polymer chain. The chain segments far removed from the graft site assume the planar zigzag conformation of the unmodified polyethylene molecule. These regular sections can pack together to form periodic three-dimensional structures associated with crystalline matter. The three-dimensional periodicity is characterized by a typical unit cell of the regular array of molecules. The unit cell of polyethylene has been determined to be orthorhombic, with cell edge dimensions of $a = 7.40$ Å, $b = 4.93$ Å, and $c = 2.53$ Å (*1*). Two planar zigzag sections are contained within the unit cell. The unit cell represents the fundamental repeating unit of the periodic structure of the crystal.

The polymeric materials form submicro-

[1] Present address: Air Products and Chemicals, Allentown, Pennsylvania 18105.

[2] To whom correspondence should be addressed.

0021-9517/80/060372-11$02.00/0

scopic plate-like crystals called lamellae. The lamellae are typically 200 to 600 Å thick and several thousand Ångströms in length and width; the chain axis of the polyethylene molecule is parallel to the small dimension of the lamella. Since this small dimension accommodates 50 to 100 repeating units, only sections of the long molecules are contained in the lamellae. Consequently, contiguous regions of chain segments packed into regular crystalline arrays may be connected by chain sections of a more coiled and random nature. The specific conformation of these noncrystalline or "amorphous" chain segments is not known.

The molecular segments spanning two lamellae are called "tie molecules." Each molecular segment within a lamella is not necessarily connected by a tie molecule to another lamella. The molecules may terminate near the surface of the lamella to produce cilia or "fringes" on the lamella. Alternatively, the molecule may fold back on itself so that a separate segment of the same molecule can reenter the lamella, thereby forming a "loop" or "fold" on the surface.

The crystal lamellae and the associated amorphous molecular segments are aggregated into a spherically symmetrical supramolecular structure or spherulite. The spherulites give rise to a texture similar to the grain structure of a metal. The spherulites in a polymer are polycrystalline, however, whereas metallic grains are essentially monocrystals. Spherulites may range from microns to centimeters in diameter.

Within a spherulite, the lamellae are arranged along radial directions which have a common center at the site of nucleation. The *b* axis direction of the crystals lies along the spherulite radius, whereas the *a* axis and *c* axis tend to be randomly oriented in the planes perpendicular to the radii. Consequently, the polymer chain axis direction (the *c* axis) is oriented perpendicular to the radial direction and therefore is tangential to the surface of the spherulite. Even though the individual lamellae are anisotropic, the spherulitic geometry produces a structural unit which is isotropic on the average. Upon deformation, the spherulites tend to become ellipsoidal. Eventually, the highly deformed spherulites are disrupted and form oriented fibrillar morphologies, with the long dimensions of the lamellae perpendicular to the draw direction.

The gross properties of a semicrystalline polymer depend upon the interactions between the crystalline and the amorphous components, as reflected by the size, shape, and relative orientations of the two components. The relative influence of each of these components depends upon the fraction and arrangement of the chain segments in each. The crystalline content (i.e., percentage crystallinity) can be obtained from precise measurements of density. The relative arrangement of the crystalline segments can be obtained by X-ray diffraction techniques; the orientation of chain segments in the amorphous regions can be deduced from measurements of birefringence. The application of these structural characterization techniques provides a means of tracking structural modifications induced by drawing the polymeric catalysts.

The dehydration of isopropyl alcohol was selected as the test reaction for determining catalytic activities of the semicrystalline polymers, since the activity for this reaction has been found to be sensitive to the structure of a polymeric catalyst (*2*): the catalytic reaction rate was reported to increase by an order of magnitude as the divinylbenzene content (crosslinking) of a sulfonated poly(styrene–divinylbenzene) ion-exchange resin catalyst was reduced from 8 to 5%. Further, the rates of alcohol dehydration reactions in these resins have been found to increase more than linearly with increasing concentration of $-SO_3H$ groups, suggesting that the dehydration reactions occur in association with clusters of hydrogen-bonded $-SO_3H$ groups; the exis-

tence of these clusters has been demonstrated by infrared spectra of functioning catalysts (*2, 3*).

EXPERIMENTAL METHODS

Permion 5010 (RAI Research Corp., Long Island, N.Y.) was prepared by γ-radiation grafting of styrene onto polyethylene film, followed by sulfonation of the styrene units with chlorosulfonic acid at room temperature. The films were obtained from RAI in the potassium salt form; they were converted into the hydrogen form by aqueous ion exchange, undergoing repeated batch contacting with 1 *N* HCl followed by washing with distilled water until the decanted solution was free of chloride ion, as indicated by the lack of formation of a precipitate upon addition of $AgNO_3$. Analysis of digested samples by Galbraith Laboratories, Knoxville, Tennessee, showed that the K^+ content was <0.1 wt%. The $-SO_3H$ group contents of the samples were determined by addition of excess 0.025 *N* NaOH solution containing 1% NaCl; after equilibration, the supernatant solution was back-titrated against 0.01 *N* HCl using phenolphthalein indicator. The samples all contained 0.83 ± 0.03 meq of $-SO_3H$ groups/g (dried under vacuum at 120°C).

The polymer films, all from the same batch and initially 0.02 cm in thickness, were cut into 10-cm-long sections and drawn in an Instron Universal Testing Instrument (Model TTCM) with a crosshead speed of 0.5 cm/min. After drawing, each sample was allowed to relax between the grips for 10 h to ensure reproducibility of structural changes. Samples were drawn to 1.75, 2.50, and 3.00 times their initial lengths. One sample was drawn and redrawn after breaking three times to induce the extreme structural variation. This sample is referred to as "repeatedly drawn."

A thermostated flow reactor system constructed of glass and stainless steel was used for measurement of catalytic activities. The equipment, described in more detail elsewhere (*4*), was modified to allow vaporized isopropyl alcohol fed from a syringe pump to be mixed in various proportions with helium diluent. The glass tubular reactor (2.0 cm in diameter and 20 cm in length) held a clamp for the coiled catalyst sample to prevent it from changing its length during operation. The reaction products flowed steadily through heated transfer lines to an on-line, heated sampling valve of gas chromatograph equipped with a Porapak N column. Products were analyzed periodically, and steady-state operation was demonstrated by the constancy of repeated analyses determining conversion. The catalysts were stable, experiencing no measurable loss of activity during these experiments.

In the kinetics experiments, the partial pressure of isopropyl alcohol reactant in helium carrier was varied from 0.01 to 0.5 atm. The alcohol feed rate varied from 0.002 to 0.06 mole/h. The repeated analysis of products by gas chromatography allowed determination of conversions with an estimated precision of ±5%. Flow rates were chosen to give low (differential) conversions, typically <3%.

The structures of the films were characterized by (1) precise density measurements to determine the volume fraction of crystalline (x_c) and amorphous ($x_a = 1 - x_c$) material; (2) by X-ray diffraction to provide information about the orientation of the chain axes in the crystalline regions; and (3) by birefringence measurements to determine the state of orientation of chain segments in the amorphous regions. All structural characterizations were carried out after the completion of the catalytic activity measurements. The applications of the experimental methods in this research are summarized below; details are given elsewhere (*5, 6*).

The percentage crystallinity of the polymer catalyst was determined by using the additive nature of intensive properties such as specific volume. The specific volume was determined from measurements of the density of the sample using a density gradi-

ent column described in *ASTM* standards (*7*).

A value for the crystalline density can be obtained from a knowledge of the unit cell dimensions and the molecular weight of the monomer contained in a unit cell: $d_c = 1.00$ g/cm^3. The density of amorphous polyethylene can only be estimated, since no completely amorphous linear polyethylene exists. A value is reported by McCready *et al.* (*8*): $d_a = 0.83$ g/cm^3.

The state of crystalline orientation was determined by measuring azimuthal intensity profiles along the 110 and 200 Debye–Sherrer rings according to procedures summarized by Alexander (*9*). The state of orientation for a given *hkl* plane of the crystal can be expressed in terms of the Herman's orientation factor, f_{hkl} (*10*)

$$f_{hkl} = \tfrac{1}{2}(3\ \langle \cos^2 \rho_{hkl} \rangle - 1) \qquad (1)$$

with

$$\langle \cos^2 \rho_{hkl} \rangle = \frac{\int_{\rho=0}^{\pi/2} I(\rho_{hkl}) \cos^2 \rho_{hkl} \sin \rho_{hkl} d\rho_{hkl}}{\int_{\rho=0}^{\pi/2} I(\rho_{hkl}) \sin \rho_{hkl} d\rho_{hkl}}, \qquad (2)$$

where I_{hkl} is the measured X-ray intensity at the azimuthal angle ρ. Intensity scans for I_{hkl} were obtained using a Picker FACS-I (Four Angle Computer System) automated X-ray diffraction system.

The Herman's orientation factor for the chain axis of the crystalline regions, $f_c(=f_{001})$, was constructed from the values obtained for the 110 and 200 intensity data via the relationship (*11*)

$$\langle \cos^2 \rho_c \rangle = 1 - 1.4439\ \langle \cos^2 \rho_{110} \rangle - 0.5562\ \langle \cos^2 \rho_{200} \rangle. \qquad (3)$$

[For random orientations, $\langle \cos^2 \rho_c \rangle = \frac{1}{3}$, so that $f_c = 0$; for perfect orientation, $\langle \cos^2 \rho_c \rangle = 1$, so that $f_c = 1$. If the chain axis is perpendicular to the draw direction (but random in the transverse plane), $\langle \cos^2 \rho_c \rangle = 0$, so that $f_c = -\frac{1}{2}$.]

The orientation factor of the chain segments in the amorphous regions, f_a, can be obtained by correcting the observed birefringence of the film for the crystalline contributions. Samuels (*12*) proposed the following relationship:

$$\Delta_T = x_c f_c \Delta_c^\circ + (1 - x_c) f_a \Delta_c^\circ, \qquad (4)$$

where Δ_T is the observed birefringence and Δ_a° and Δ_c° are the "intrinsic" birefringences of the amorphous and crystalline components, respectively.

The overall birefringence was determined from retardation measurements obtained under a Leitz Orthoplan polarizing microscope using tungsten light. Retardations were matched against an Olympus Compensator of a fourth-order Bereck variety. Values of the intrinsic birefringence Δ_a° and Δ_c° are required for the determination of f_a. The procedures used to obtain these values from bond polarizabilities are discussed elsewhere (*5*, *6*).

The polymer samples were examined at a magnification of 40,000× with a scanning electron microscope equipped with an energy dispersive X-ray analyzer (EDAX) to obtain information concerning structural changes induced by drawing. Samples for microscopy were coated with a gold layer, 100–200 Å in thickness. The EDAX results provided a measure of the $-SO_3H$ group distribution (*5*).

RESULTS AND DISCUSSION

The catalysis experiments showed that isopropyl alcohol underwent the expected conversion in the presence of the sulfonated polymers, giving only propylene and water as the observed products. The conversions of alcohol were low (typically <3%), and plots of conversion vs inverse space velocity were linear, passing through

the origin (*5*); these results demonstrate that the conversions were differential, so that reaction rates were determined directly. The rate data, obtained at 100°C and 1 atm, are summarized in Fig. 1.

Rates of isopropyl alcohol dehydration per $-SO_3H$ group determined with single polymer films were indistinguishable from rates determined with a pair of the same films sandwiched together. These results indicate that rates were independent of the characteristic diffusion length and were therefore not influenced by diffusion.

For each catalyst film, the rate reached a maximum at an isopropyl alcohol partial pressure of about 0.1 atm—in agreement with results observed with sulfonated poly(styrene–divinylbenzene) resin catalysts, which had approximately the same activity per $-SO_3H$ (*2*). The data of Fig. 1 demonstrate the sensitivity of the catalytic activity to the structural changes induced by drawing: As the draw ratio (final length/initial length) was increased to 2.50, the activity at a given alcohol partial pressure increased, but as the draw ratio was further increased, the activity decreased.

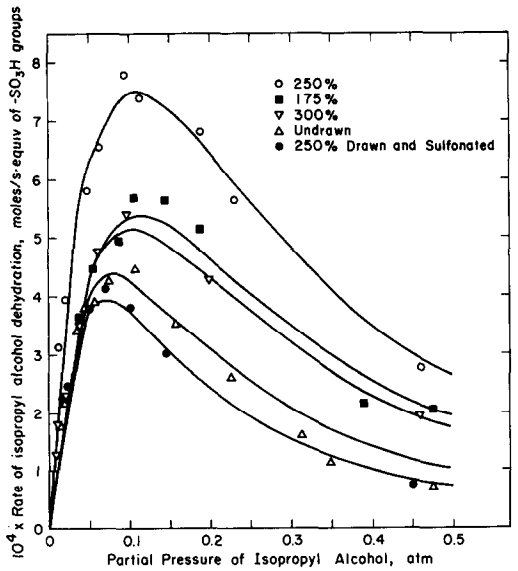

FIG. 1. Kinetics data for dehydration of isopropyl alcohol catalyzed by variously drawn films of sulfonated polyethylene-graft styrene at 100°C and 1 atm. The curves are the predictions of Eq. (9) with the parameter values of Table 2.

TABLE 1

Summary of Structural Parameters

Catalyst sample	Density (g/cm³)	f_c	f_a
Undrawn	1.050 ± 0.001	0.03	0.13
1.75 draw ratio	1.050 ± 0.001	0.12	0.21
2.50 draw ratio	1.050 ± 0.001	0.34	0.18
3.0 draw ratio	1.050 ± 0.001	0.68	0.05
Repeatedly drawn	1.050 ± 0.001	0.80	0.08

Electron micrographs (with a resolution of about 100 Å), taken before and after drawing, as well as before and after the catalysis experiments, showed no evidence of formation of microcracks (*5*). These results show that the observed increases in catalytic activity produced by drawing did not result from formation of new surface sites.

The structural data for each catalyst film are summarized in Table 1. These results show that the amorphous orientation factor, f_a, passes through a maximum with increasing draw ratio, as does the catalytic activity. As expected, the crystalline orientation factor increased with increasing draw ratio. The density (and hence the percentage crystallinity) remained constant.

Location of Graft Sites

Catalytic performance depends on the spacing and interaction of the catalytically active $-SO_3H$ groups within the polymer film, which are governed by the locations of the styrene grafts and the number of styrene monomers per grafted side chain. The reaction kinetics of the radiation-induced grafting of styrene onto polyethylene film was studied by Wilson (*13*), who reported initiation, propagation, and termination rate constants. Rate constants for free-radical polymerization of styrene are also available (*14*). Comparison of these values shows that the rate of grafting of styrene monomer onto polyethylene film is approximately two orders of magnitude higher than

that of polystyrene chain formation. This result implies a low probability for chain formation at the graft site. Further, chain formation followed by grafting onto the polyethylene backbone is unlikely since the bulky chain could not migrate rapidly to the reaction site. Consequently, we infer that the predominant form of the grafted styrene is a monomeric unit. The subsequent sulfonation occurs predominantly at the para position of the grafted styrene.

The monomeric styrene graft is too large to be accommodated within the free volume of the densely packed crystalline regions. Therefore, we infer that the pendant styrenes on the polyethylene chains are present in the amorphous regions. This inference is supported by the dynamic mechanical spectra of the films: The γ-relaxation peak observed in the tan δ spectrum is associated with the amorphous phase (*15*); consequently, any shifts in the position of this peak can be related to events occurring within the amorphous phase. The γ-relaxation peak was observed at $-119°$ for polyethylene film, at $-124°$ for polyethylene film grafted with styrene, and at 130° for polyethylene film grafted with sulfonated styrene. The corresponding "crystalline" relaxation peaks were unchanged by grafting and sulfonation.

Density measurements showed that the initial semicrystalline polymer had 57 vol% crystalline material, a typical value for linear polyethylene. Using these results and an estimated density of amorphous regions (modified by the grafted styrene), we estimate that sulfonation of all the styrene units would give ~ 1 meq of $-SO_3H$ groups/g of catalyst, which is nearly equal to the measured values of 0.83. These results imply that styrene grafted in the amorphous regions did not change the crystallinity of polyethylene and that all the pendant styrenes were sulfonated.

The foregoing results provide strong support for the contention that the catalytic sites were excluded from the interior crystalline regions. Nonetheless, the catalytic sites could be associated with the crystalline material by attachment to the folds on the surfaces of the lamellae. Grafting of styrene preferentially onto the crystalline surfaces is expected from energy considerations. The grafting proceeds via a free-radical mechanism involving the polyethylene chain and styrene molecules, with the energy required for the free-radical formation supplied by γ-radiation. McMahon *et al.* (*16*) showed that folds on the crystalline surface are highly strained, having a conformational energy of approximately 20 kcal/mole as compared with a conformational energy of approximately 5 kcal/mole of a chain in an amorphous region. The high-energy fold sites promote grafting initially at the crystalline surfaces. However, only a limited number of the bulky styrene molecules can be accommodated at neighboring fold sites. Consequently, we infer that after some undetermined coverage of the crystalline surfaces has been achieved, the grafting reaction progresses into the lower-energy sites of the amorphous regions. Therefore at sufficient styrene concentrations, graft sites will be located both on crystalline surfaces and in amorphous regions.

On the basis of the observed influence of draw-induced structural changes on catalytic performance and the arguments assigning the locations of the $-SO_3H$ groups, we proceed by interpreting these results in the context of the previously cited models of the catalytic sites, namely, a hydrogen-bonded cluster of several $-SO_3H$ groups or, alternatively, widely spaced $-SO_3H$ groups, which act separately (*2, 3*). Following the development of this model on the molecular scale, we take account of the physical influences of the structures and orientation of the crystalline and amorphous domains on catalytic performance.

Catalytic Sites

The strong similarity between the present rate data and those obtained with amorphous (gel-form), sulfonated poly(styrene–

divinylbenzene) catalysts (*2*) suggests that the previously proposed (*2, 3*) molecular model of the catalytic site applies as well to the semicrystalline polymer. According to this model, when anhydrous $-SO_3H$ groups in an amorphous polymer matrix are present near each other, they form a tightly hydrogen-bonded network, with each $-SO_3H$ group acting as both a proton donor and a proton acceptor. To be catalytically converted, alcohol molecules must break into the network, forming a hydrogen-bonded intermediate with a structure such as the following:

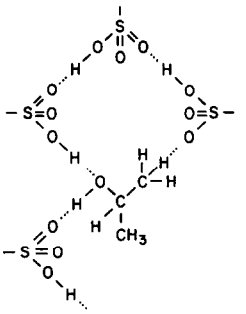

The dehydration reaction can result from a concerted proton transfer within this network. This suggestion is one limiting case of the model, accounting for the minimum spacing of the $-SO_3H$ groups. In the other limiting case (*5*), the groups are too far apart in the matrix to allow the hydrogen-bonded network to form; then the acid groups may act alone (but less efficiently) to form a *s*-propyl carbonium ion, which can then back-donate a proton to give propylene. In the (intermediate) case of maximum catalytic activity, the acid groups have an optimum spacing—allowing alcohol to compete successfully with $-SO_3H$ groups in bonding with other $-SO_3H$ groups—while the network remains intact and the concerted proton transfer process is still allowed. When more than the optimum amount of alcohol is present, it inhibits reaction by occupying too many positions, breaking up the network and hindering the concerted proton transfers (*2*).

The present data are consistent with this model, showing (i) the inhibition of reaction by alcohol at partial pressures $\gtrsim 0.1$ atm (Fig. 1) and showing (ii) an initial increase in catalytic activity as the spacing of the acid groups is increased by drawing and then a decrease in activity as the spacing of the acid groups is increased beyond the optimum by further drawing. We elaborate on the first point, accounting quantitatively for the inhibition by alcohol, and then, to explain the second point, consider the structural effects of drawing on the polymer microstructure.

TABLE 2

Summary of the Kinetic Data: Parameter Values for Eq. (9)

Catalyst sample	$k \times 10^{3a}$ (moles/s · eq of $-SO_3H$ groups)	$K_A{}^a$ (atm^{-1})	Maximum rate $\times 10^{4a}$ (moles/s · eq of $-SO_3H$ groups)
Undrawn	4.1 ± 0.4	4.3 ± 0.2	4.2 ± 0.3
1.75 draw ratio	5.1 ± 0.7	3.0 ± 0.2	5.6 ± 0.3
2.50 draw ratio	7.1 ± 1.0	3.1 ± 0.2	7.5 ± 0.3
3.0 draw ratio	4.9 ± 0.4	3.2 ± 0.1	5.3 ± 0.3
Repeatedly drawn	2.3 ± 0.3	3.9 ± 0.2	2.5 ± 0.1

[a] Data are reported with 95% confidence limits.

Analysis of the rate data (*5*) has shown that the following equation provides a better fit than any other of comparable complexity:

$$r = \frac{k' P_A}{(1 + K_A P_A)^4}. \qquad (5)$$

This equation provides a good fit of the data for each draw ratio, as shown in Fig. 1. The parameter values, determined by the standard Marquardt nonlinear least-squares fitting criterion (*17*), are collected in Table 2.

The rate equation can be developed from a simple model of the catalytic process: We assume that the rate-determining step involves the combination of an alcohol molecule which is bonded to one $-SO_3H$ group with a cluster of three neighboring $-SO_3H$ groups; we assume that the bonding (adsorption) of alcohol to the groups is described by the Langmuir isotherm, as has

been observed for ethyl alcohol and sulfonated poly(styrene–divinylbenzene) under similar conditions (*18*). Therefore

$$\theta_A = \frac{K_A P_A}{1 + K_A P_A} \tag{6}$$

$$\theta_V = \frac{1}{1 + K_A P_A} \tag{7}$$

$$r = k\theta_A \theta_V^3 \tag{8}$$

$$r = \frac{kK_A P_A}{(1 + K_A P_A)^4}. \tag{9}$$

The quantity k' of Eq. (7) is identified as kK_A.

This model is clearly an oversimplification; nonetheless, it fits the data for each catalyst well and represents the important idea that the catalytic sites involve clusters of several $-SO_3H$ groups. The values of the empirical parameters (Table 2) show an opposite dependence on draw ratio; k passes through a maximum, while K_A passes through a minimum with increasing draw ratio. These parameters, if interpreted literally, represent the rate constant for the reaction and adsorption equilibrium constant of alcohol, respectively. In this context, the dependence of k on the draw ratio is consistent with the cluster structure; the dependence of K_A on the draw ratio remains unexplained.

Structure–Deformation Model

Linear polyethylene, which provides the support for the catalytically active $-SO_3H$ groups, has been the subject of numerous studies dealing with macroscopic deformation as well as microscopic morphological changes. Models of microstructural changes at the level of lamellae or spherulites have provided mechanisms for relating microstructural changes to macroscopic deformations (*19, 20*). Similar models are appropriate to explain the changes in the catalytic activity of the polymers brought about by drawing. The interpretation of the observed structural effects on catalytic performance in terms of structure–deformation models is briefly summarized below. The detailed justifications for the models are given elsewhere (*5, 6*).

The envisioned structural changes associated with various stages of deformation are schematically illustrated in Fig. 2. Structures A through E show the proposed microstructural changes taking place with increasing elongation. Structures B and C are related to the destruction of microspherulites, and D and E are related to deformations of the crystalline and amorphous domains contained in the microfibrillar structure created by extensive elongation.

Structure A, representing the undrawn catalyst, shows a random and closely packed amorphous phase containing $-SO_3H$ groups. On a morphological level, the spherulites are undeformed and distributed throughout the sample.

Structure B represents the microstructure of the sample subjected to small deformations (e.g., 10%). During this stage a reorientation of crystalline and amorphous domains takes place within the deforming spherulite. This reorganization depends upon the positions of the lamellae with respect to the draw direction. At these low elongations, crystalline orientation is not significant, and extension of the amorphous domain is accompanied by slipping of the lamellae rigidly past each other. This rearrangement of polymer segments within the amorphous regions causes changes in the placement of sulfonic acid groups and, hence, provides a basis for explaining the changes observed in catalytic activity resulting from drawing. Upon further elongation, crystalline regions become increasingly aligned in the draw direction. The amorphous phase extensions and rearrangements of the catalytic sites during this stage of drawing are accompanied by slip and tilting of the lamellae. These are consistent with the X-ray diffraction data. Structure C represents an intermediate state in which crystalline chain segments are approaching alignment in the draw direction.

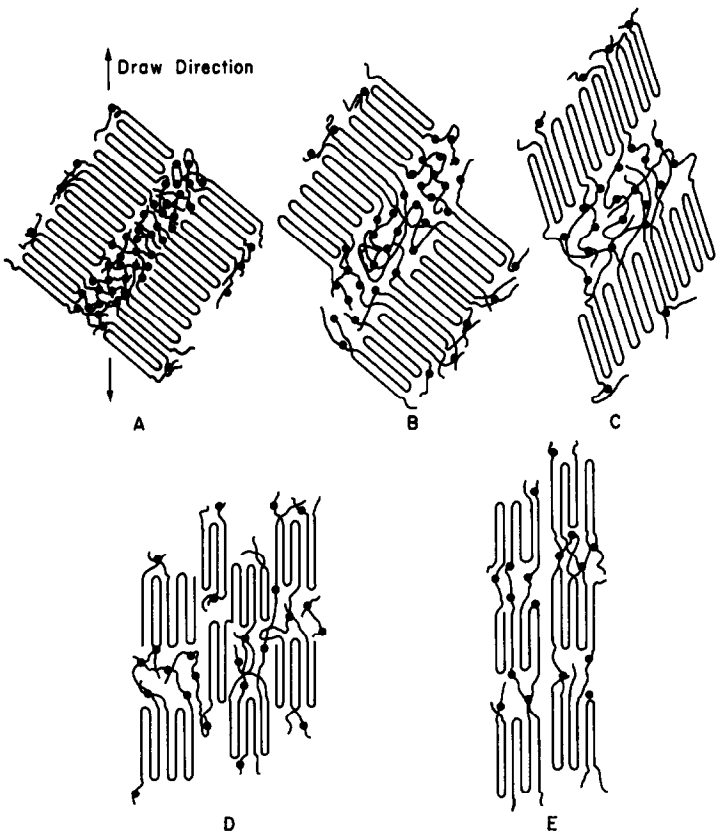

FIG. 2. Structural model of semicrystalline sulfonated polyethylene-graft styrene at various elongations. Rearrangements at moderately low deformations: (A) undrawn state; (B) lamellar sliding and expansion of amorphous phase; (C) crystalline orientation and further expansion of amorphous phase; rearrangements at moderately high deformations; (D) crystalline cleavage and amorphous orientation; (E) microfibril formation and spherulite breakup with high degree of amorphous orientation. The dots represent $-SO_3H$ groups.

At very high elongations, crystal blocks (i.e., crystallites) are pulled out of the lamellae, as illustrated in Structure D. Upon further drawing, these blocks become aligned along the draw axis, and a microfibrillar structure, E, is obtained. Structures D and E can occur only at extreme elongations and therefore also have high degrees of amorphous orientation. The low values observed for the amorphous phase ($f_a \sim 0.1$) indicate that highly oriented amorphous structures D and E were not encountered at the draw ratios used in the present study. The data indicate the presence of structures intermediate between B and C. Therefore, all the changes taking place in the amorphous phase are inferred to result from sliding and tilting of lamellae.

This model of the polymer structure is consistent with the molecular model of the catalytic sites. Rearrangement of $-SO_3H$ groups is responsible for the increase in catalytic reaction rates up to draw ratios of 2.50 and for the decline upon further drawing. In Structure A, the $-SO_3H$ groups are clustered and do not allow the efficient formation of the reaction intermediates. Upon drawing, the amorphous region is rearranged and $-SO_3H$ groups are broken apart, giving rise to higher catalytic activities. Beyond the optimum extension, the

separation of the $-SO_3H$ groups beyond the hydrogen-bonding distance reduces their participation in the reaction, and consequently the activity declines. It was observed that a polymer film drawn first and then sulfonated was less active than one sulfonated prior to drawing. Evidently, drawing before sulfonation allows higher crystalline orientation and hence more separation between grafts in the amorphous domain. Thus, after sulfonation the distances between $-SO_3H$ groups may be greater than the hydrogen-bond distance, so that the observed catalytic activity is lower than that of a presulfonated film drawn to the same elongation.

As pointed out previously, the $-SO_3H$ groups are distributed between the folds on the surfaces of the lamellae and the random chains in the amorphous domains. For the concerted reaction to proceed, a cluster of $-SO_3H$ groups is required. Thus, reactions can proceed between (i) two crystalline surfaces, (ii) amorphous chains and one crystalline surface, (iii) sites on the same crystalline surface, and (iv) within the amorphous regions.

For reactions to take place between the surfaces of two lamellae, the separation between the lamellae should be small enough for the reactant alcohol to bridge the $-SO_3H$ groups. Recent work (*8*) has shown that for melt-crystallized linear polyethylene, the average distance between two lamellae is approximately 50 Å; this is too large a separation for the appropriate bonding between alcohol and $-SO_3H$ groups to take place. Accordingly, we infer that the major contributions to catalytic activity arise from clustering of $-SO_3H$ groups between (i) sites on the same lamellar surface, (ii) lamellar surface–amorphous chain sites, and (iii) amorphous chain–amorphous chain sites. Clusters involving sites on the same lamellar surface would be unaffected by deformation; therefore the combinations (ii) and (iii) provide the catalytic sites having structures sensitive to deformation.

APPENDIX: NOTATION

a, b, c	unit cell dimensions
d	density, g/cm^3
Δ°	"intrinsic" birefringence
Δ_T	observed birefringence
f_{hkl}	Herman's orientation factor for the *hkl* plane
I	X-ray intensity
K	temperature-dependent parameter in rate equation (adsorption equilibrium constant)
k	reaction rate constant, dimensions of r
k'	kK_A
P	partial presure, atm
r	reaction rate, moles per equivalent of $-SO_3H$ groups per second
ρ	angle between chain axis and draw direction
tan δ	loss factor (δ: plane angle between stress and strain)
θ	fraction of catalytic sites
x	volume fraction

Subscripts

a	amorphous
A	alcohol
c	crystalline
v	vacant

ACKNOWLEDGMENT

We thank RAI Corporation for providing the catalyst samples.

REFERENCES

1. Bunn, C. W., *Trans. Faraday Soc.* **35,** 482 (1930).
2. Thornton, R., and Gates, B. C., *J. Catal.* **34,** 175 (1974).
3. Gates, B. C., Wisnouskas, J. S., and Heath, H. W., Jr., *J. Catal.* **24,** 320 (1972).
4. Swabb, E. A., and Gates, B. C., *Ind. Eng. Chem. Fundam.* **11,** 540 (1972).
5. Cooper, C. A., Ph.D. Thesis, University of Delaware, 1979.
6. Cooper, C. A., McCullough, R. L., Gates, B. C., and Seferis, J. C., to be published.
7. Payne, N., and Stephenson, C. E., *ASTM Mater. Res. Stand.* **4**(1), 3 (1964).
8. McCready, M. J., Schultz, J. M., Lin, J. S., and Hendricks, R. W., *J. Polym. Sci. Polym. Phys.*, submitted for publication.

9. Alexander, L. E., "X-ray Diffraction Methods in Polymer Science." Wiley–Interscience, New York, 1969.
10. Hermans, J. J., Herman, P. H., Vermaas, D., and Weidinger, A., *Rec. Trav. Chim.* **65,** 427 (1946).
11. Wilchinsky, Z. W., *J. Appl. Phys.* **30** 792 (1959); **31,** 1969 (1960).
12. Samuels, R. J., "Structured Polymer Properties." Wiley, New York, 1974.
13. Wilson, J. E., *J. Macromol. Sci. Chem.* **5,** 777 (1971); **9,** 609 (1975); **10,** 1441 (1976).
14. Mark, H. F., and Gaylord, N. G. (Eds.), "Encyclopedia of Polymer Science and Technology." Wiley, New York, 1972.
15. Gray, R. W., and McCrum, N. G., *J. Polym. Sci. A-2* **7,** 1329 (1969).
16. McMahon, P. E., McCullough, R. L., and Schlegel, A. A., *J. Appl. Phys.* **38,** 4123 (1967).
17. Marquardt, D. W., *J. Soc. Ind. Appl. Math.* **11,** 431 (1963).
18. Kabel, R. L., and Johanson, L. N., *Amer. Inst. Chem. Eng. J.* **8,** 621 (1962).
19. Meinel, G., and Peterlin, A., *J. Polym. Sci.* **9,** 67 (1971).
20. Schultz, J. M., "Polymer Materials Science." Prentice–Hall, Englewood Cliffs, N.J. 1974.